Hindawi
Advances in Civil Engineering
Volume 2019, Article ID 2563183, 15 pages
https://doi.org/10.1155/2019/2563183

Research Article

Stability Assessment of Landslides in Dahuaqiao Reservoir Area Based on Back Analysis of Slope Monitoring

Yu-xiao Wang[1,2] **Yu-jie Wang**[3] **Long Jiang**[3] **Ping Sun**[3] **Xingchao Lin**[3] **and Shouyi Li**[1]

[1]*College of Water Conservancy and Hydropower Engineering, Xi'an University of Technology, Xi'an, Shaanxi 710048, China*
[2]*Qinghai Engineering Construction of Huanghe Hydropower, Xining, Qinghai 810003, China*
[3]*State Key Laboratory of Simulation and Regulation of Water Cycle in River Basin, China Institute of Water Resources and Hydropower Research, Beijing 10048, China*

Correspondence should be addressed to Yu-jie Wang; geyjwang@foxmail.com

Received 16 March 2019; Revised 4 June 2019; Accepted 10 June 2019; Published 4 July 2019

Academic Editor: Jian Ji

Dahuaqiao Hydropower Station is the sixth cascade hydropower project on the upper stream of the Lancang River, and a number of slope instabilities were found in the reservoir area before reservoir impoundment. The reservoir impoundment and fluctuation of the reservoir water level generally reactivate these potential slope failures or trigger new ones. Therefore, how to cope with the influence of these slope failures on dam safety has always been the focus of attention. However, it is unwise to stabilize all these potentially instable slopes by remedial measures. Based on a two-parameter and four-level back analysis method proposed in this paper, reasonable measures for landslide management are suggested on the basis of the in situ monitoring results and back analysis of geomaterial strength parameters.

1. Introduction

Reservoir impoundment generally induces the large-scale slope instability in the reservoir area and has a high probability to lead to slope failures. How to alleviate the influence of slope failures on dam safety has been always the focus of attention [1, 2]. Thus, reservoir designers need to solve technical problems like assuring the safety of potentially instable landslides and reducing the adverse impact on the dam safety during reservoir filling with necessary engineering measures and additional landslide monitoring approaches. However, according to the design criterion, a colossal amount of budget is needed to satisfy the stability requirement of large-scale landslides after reservoir filling, which is economically infeasible. Therefore, a premonitoring program for the landslides is commonly adopted to ensure a relatively low probability of failure and carry out corresponding landslide forecasting. The landslide forecasting results determine whether further stabilization measures are necessary.

Landslide forecasting is still a significant challenge and the research focus in natural hazard risk mitigation [3–10]. The development of the landslide forecasting can be classified into three stages. First, Saito proposed semiempirical methods to estimate the timing of slope failure based on the monitoring displacement data acquired via different techniques [3], after which, a number of landslide forecasting models and methods, such as the harmonic analysis method [4], the orthogonal polynomials-based best approximation model [5], the Markov forecasting model [6], the gradient sinusoidal model, and the grey theory [7], have been developed successively. Second, with the establishment of nonlinear theory in the twentieth century and its wide application in various fields, nonlinear theory was introduced to landslide forecasting and used to elaborate the complicated spatiotemporal evolution process of slope deformation [8–10]. Third, with the development of system science and intelligence, various methods have been combined instead of using a single approach for landslide warning and forecasting, such as the expert system based on

geologists and geotechnical engineers' expertise, the grey neural network prediction model, and the variable weighted joint forecasting method based on grey prediction, model prediction, and synergetic prediction techniques [11–13].

According to the monitoring items, landslide monitoring can fall into three categories, i.e., deformation monitoring, governing factors monitoring, and induced factors monitoring. Researches show that there are many local early warning systems for rockslides, deep-seated complex landslides, and debris flows at specific sites where geotechnical instruments provide detailed information [14, 15]. Based on the monitoring results, the relationship between the stability state indicated by the factor of safety and the actual deformation state indicated by deformation velocity/rate may be obtained [16], and this has become a research focus recently [17–20]. The philosophy may be explained as (1) based on the monitoring results of deformation and rainfall, the effects of pore water pressure (or water level in slope) and deformation evolution on slope stability can be evaluated after rainwater infiltration; (2) based on the actual pore water pressure, the instantaneous factor of safety can be calculated or renewed through the commonly used limit equilibrium methods; (3) with the empirical relationship between the factor of safety and the deformation rate along the slip surface, we can decide whether to take further engineering stabilization measures or insist on the original monitoring program only.

Dahuaqiao Hydropower Station is the sixth cascade hydropower project on the upstream of Lancang River. This project has one roller-compacted concrete gravity dam with the maximum height of 106 m and a reservoir whose total storage is 293 million m^3. The reservoir area, where the river valleys are mostly V-shaped, is featured with a high and medium mountain canyon landform (see Figure 1). Previous geological investigation results show that 17 large landslide-prone areas were found in the 35 km long reservoir area close to the dam, covering a volume of 8000×10^4 m^3 (see Table 1). Besides, these landslides are still in slow movement before reservoir filling, so the potential failure of landslides during the filling or water level change of reservoir will directly damage the residential villages and buildings or even induce large water waves which affect shipping and dam safety. Therefore, it is quite necessary to predict and prevent the instability damage resulted from landslides.

It is infeasible to stabilize all the landslides in the reservoir area due to the limited economic or technological conditions. Therefore, the overall monitoring and forecasting of specific landslide play an important role in preventing and mitigating landslide disasters. Based on the detailed analysis on the topographical and geological conditions of landslides in the Dahuaqiao reservoir area, the design agency made a targeted design for slope monitoring and performed all-round monitoring. This paper attempts to propose a back analysis approach to establish the relationship between the measured deformation of slopes and the shear strength parameters along slip surfaces. Afterwards, a further stability analysis is conducted based on the back-analyzed parameters. For generalization, the following analysis is conducted on two selected landslides, one is located at the left bank, namely, Cangjiangqiao landslide, and the other one is located at the right bank, i.e., Dahua landslide.

2. Engineering Geological Conditions

The Lancang River stretches approximately from the south to the north in the reservoir area near the dam site, and the mountain top elevation between both sides falls largely in the range of 2,700 to 3,600 m, with a relative height difference of 1,300 to 2,500 m. Most river valleys in the reservoir area are V-shaped, showing a high and medium mountain canyon landform; the water course twists and turns, and the slopes of both sides generally range between 25° and 50°. Exposed lithology consists of Permian System, Triassic System, Jurassic System, and Cretaceous System, among which the claret slate of Jurassic System is the most advanced; volcaniclastic rock of Triassic System is exposed only on the tail end of the reservoir; and the slate and sandstone of Cretaceous System are in the opening section. The typical geological profiles of Dahua and Cangjiangqiao landslides in the reservoir area are shown in Figure 2.

3. Analysis on the Monitoring Results of Cangjiangqiao and Dahua Landslides

3.1. Monitoring Scheme. To study the spatiotemporal evolution trend of deformation of landslide masses, monitoring schemes were worked out, respectively, for Cangjiangqiao and Dahua landslides. Figure 3 shows the layout of monitoring design. In Figure 3, abbreviations of CJQ and DH are designated for Cangjiangqiao and Dahua landslides, respectively. Four monitoring sections were arranged for Cangjiangqiao and Dahua landslides, respectively, and each monitoring section was installed with the following monitoring devices: (1) 4 to 5 GPS observation pillars for monitoring surface deformation; (2) 4 to 5 deep matrix displacement meters for monitoring internal deformation of landslide; (3) 5 to 6 surface joint meters for monitoring surface crack deformation of landslide; (4) 4 to 5 deep pore water pressure gauges for monitoring the ground water level of landslide.

3.2. Analysis on Monitoring Data. Due to space limitation, only variation of inclination results with time and space at elevations 1,710 m, 1,660 m, and 1,560 m for monitoring section CJQ-3-3 and elevations 1,710 m, 1,650 m, 1,550 m, and 1,480 m for section DH-2-2 is shown in Figures 4 and 5.

Figure 4 shows that there is a obvious slip surface at the depth of 20 m for the Cangjiangqiao landslide, and the deformation increases with time and decreases with the depth. In addition, a maximum value of 95 mm is recorded for the cumulative horizontal displacement from November 17, 2015 to June 7, 2016. Similar to Cangjiangqiao landslide, the deformation of Dahua landslide also decreases with the depth (see Figure 5). However, deformation data shown in Figure 5 indicate that there were

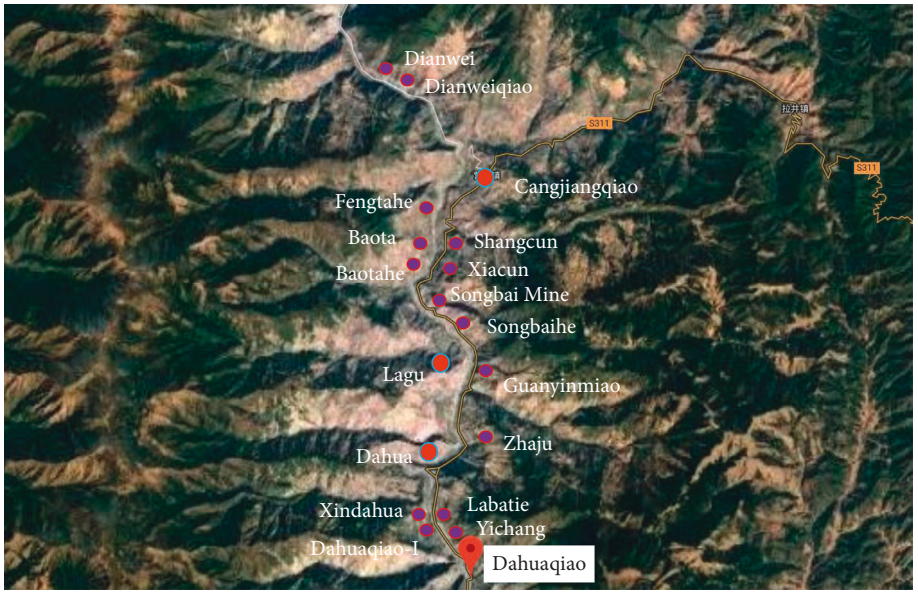

Figure 1: Landslide topography of Dahuaqiao Hydropower Station reservoir area.

Table 1: Main characteristics of the 17 landslide-prone areas in Dahuaqiao reservoir area.

Name	Location	Distance to dam (km)	Distribution elevation (m)		Volume ($*10^4$ m^3)
			Toe	Crown	
Yichang	Left bank	1.5	1498	1890	800
Dahuaqiao-I	Right bank	2.8	1410	1550	100
Labatie	Left bank	3.0	1470	1650	400
Xindahua	Right bank	3.8	1415	1580	150
Dahua	Right bank	5.1	1410	1870	4800
Zhaju	Left bank	6.8	1420	1660	150
Lagu	Right bank	12.8	1430	2000	5800
Guanyinmiao	Left bank	12.8	1430	1675	150
Songbaihe	Left bank	14.3	1435	1600	330
Songbai mine	Left bank	18.5	1450	1625	450
Baotahe	Right bank	19.0	1445	1600	320
Xiacun	Left bank	19.7	1450	1600	350
Baota	Right bank	20.1	1450	1600	300
Shangcun	Left bank	20.3	1450	1700	100
Fengtahe	Right bank	21.4	1440	1600	1300
Cangjiangqiao	Left bank	24.3	1450	1600	500
Dianweiqiao	Left bank	33.5	1470	1625	200
Dianwei	Left bank	34.5	1470	1600	600

several slip zones for Dahua landslide, along which slow creep movement is developing dynamically. However, the maximum horizontal cumulative displacement is up to 200 mm for Dahua landslide.

4. Back Analysis of Strength Parameters along Slip Surface

4.1. Establishment of Back Analysis Module. Slope deformation is a complicated process of interaction between the external agencies like precipitation, impoundment, reservoir water level fluctuation, and other human activities and the internal agencies like physical and mechanical characteristics of slope mass. In this paper, it is assumed that reservoir banks deform during reservoir filling and water level fluctuation mainly contributes to deterioration or variation of strength parameters of the slip surface (namely, strength parameters are reduced continuously). Thus, the strength parameters of the slip surface may be back analyzed by considering actual deformation state indicated by the various monitoring data. The detailed back analysis procedures (hereinafter referred to as two-parameter and four-level method) are as follows:

(1) Selecting a typical cross section such as cross section CJQ-3-3 for Cangjiangqiao landslide and DH-2-2 for Dahua landslide

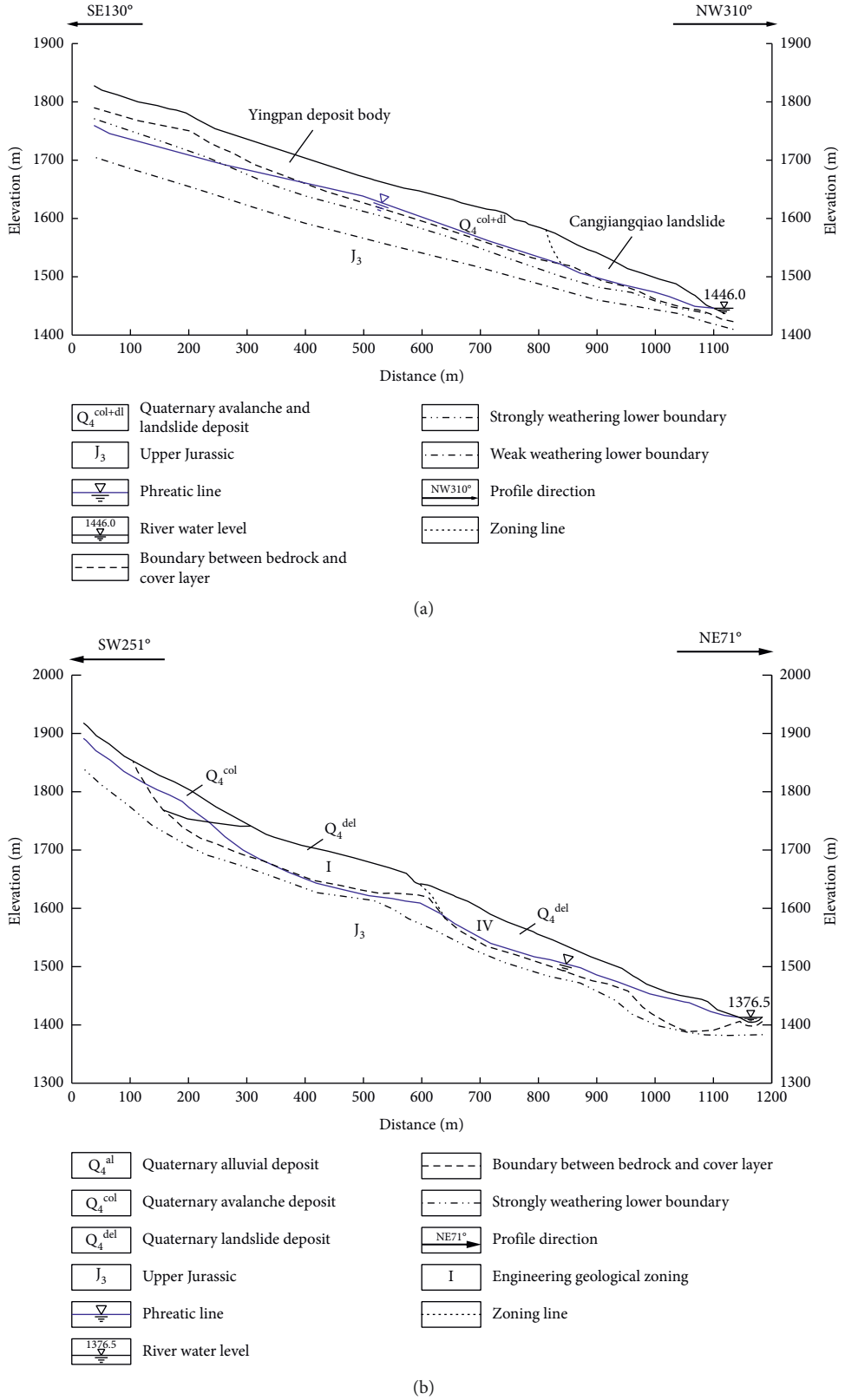

Figure 2: Typical engineering geological profiles of Cangjiangqiao and Dahua landslides. (a) Cangjiangqiao landslide. (b) Dahua landslide.

(2) Considering that the strength parameters will be deteriorated when a landslide mass is subject to external and internal agency, selecting a range of cohesion c and internal friction angle ϕ of the slip surface (hereinafter referred to as two-parameter in this paper) to be back analyzed by

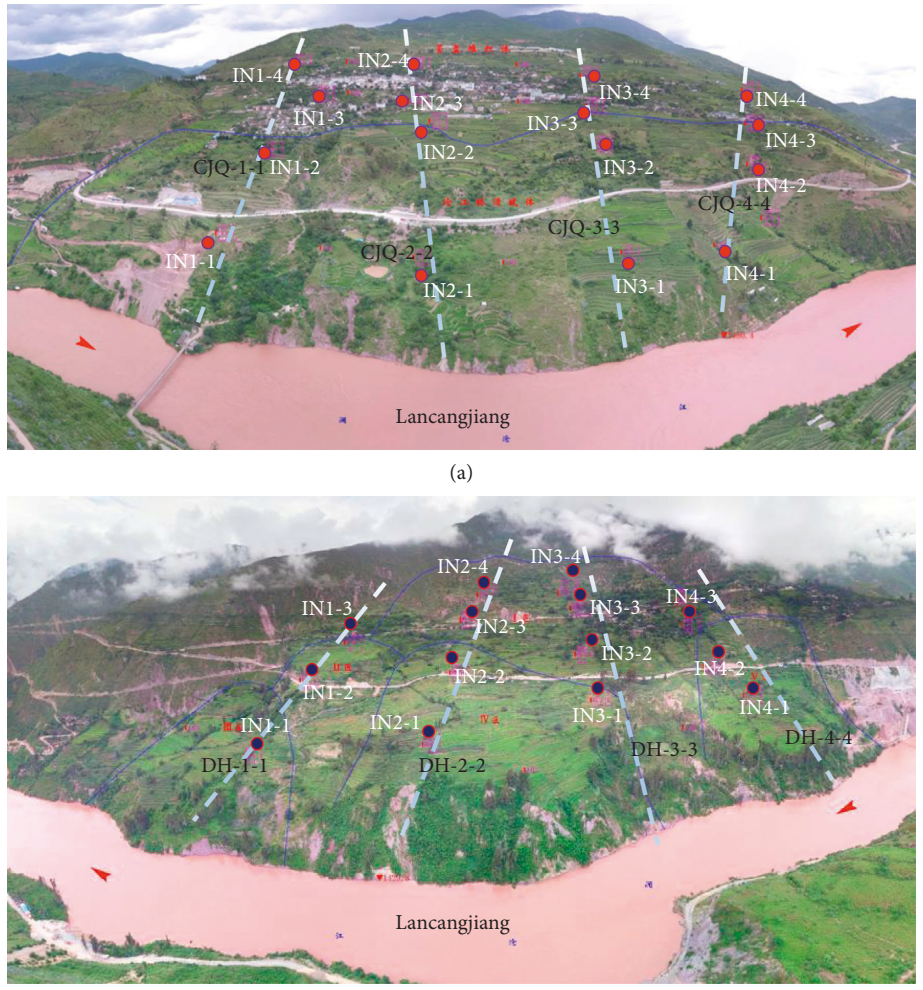

Figure 3: Schematic diagram of monitoring plan for Cangjiangqiao and Dahua landslides. (a) Cangjiangqiao landslide (left bank). (b) Dahua landslide (right bank).

(3) Quartering the range of c and ϕ (referred to as four-level in this paper) into 16 groups of c and ϕ

(4) Constructing a finite element model for the selected cross section of landslide and obtaining 16 calculated displacement values at monitoring points for each group/combination of c and ϕ through finite element analysis

(5) Obtaining best-fitting values of c and ϕ by comparing the 16 calculated displacement values with the measured one

According to the field investigation and laboratory test results, the landslide numerical model parameters selected are shown in Table 2.

4.2. Two-Parameter and Four-Level Setup. To ensure the effect and rationality of back analysis of strength parameters along slip surface, the maximum and minimum values of strength parameters (c and ϕ) related to slip surface were set according to the following principles:

(1) The strength parameters of slope mass above the slip surface are fixed during back analysis of strength parameters along the slip surface and the values are listed in Table 2.

(2) Generally, the lower bound (the minimum) of strength parameters along slip surface (c and ϕ) are set to ones of weak seam (for example, $\phi = 11.3^{\circ}$; $c = 10$ kPa). When these parameters are put into the finite element model and the finite element analysis starts, $\phi = 11.3^{\circ}$; $c = 10$ kPa are the minimum values of strength parameters for the two-parameter and four-level method, if the numerical calculation can converge (the sliding mass is in or close to limit state). In case that $\phi = 11.3^{\circ}$ and $c = 10$ kPa cannot make the finite element analysis converge, the initial values are increased so that the numerical calculation can converge. These values should be the minimum values of strength parameters along slip surface for the case of numerical calculation divergence.

(3) The upper bounds (the maximum) of strength parameters along the slip surface are assigned to values

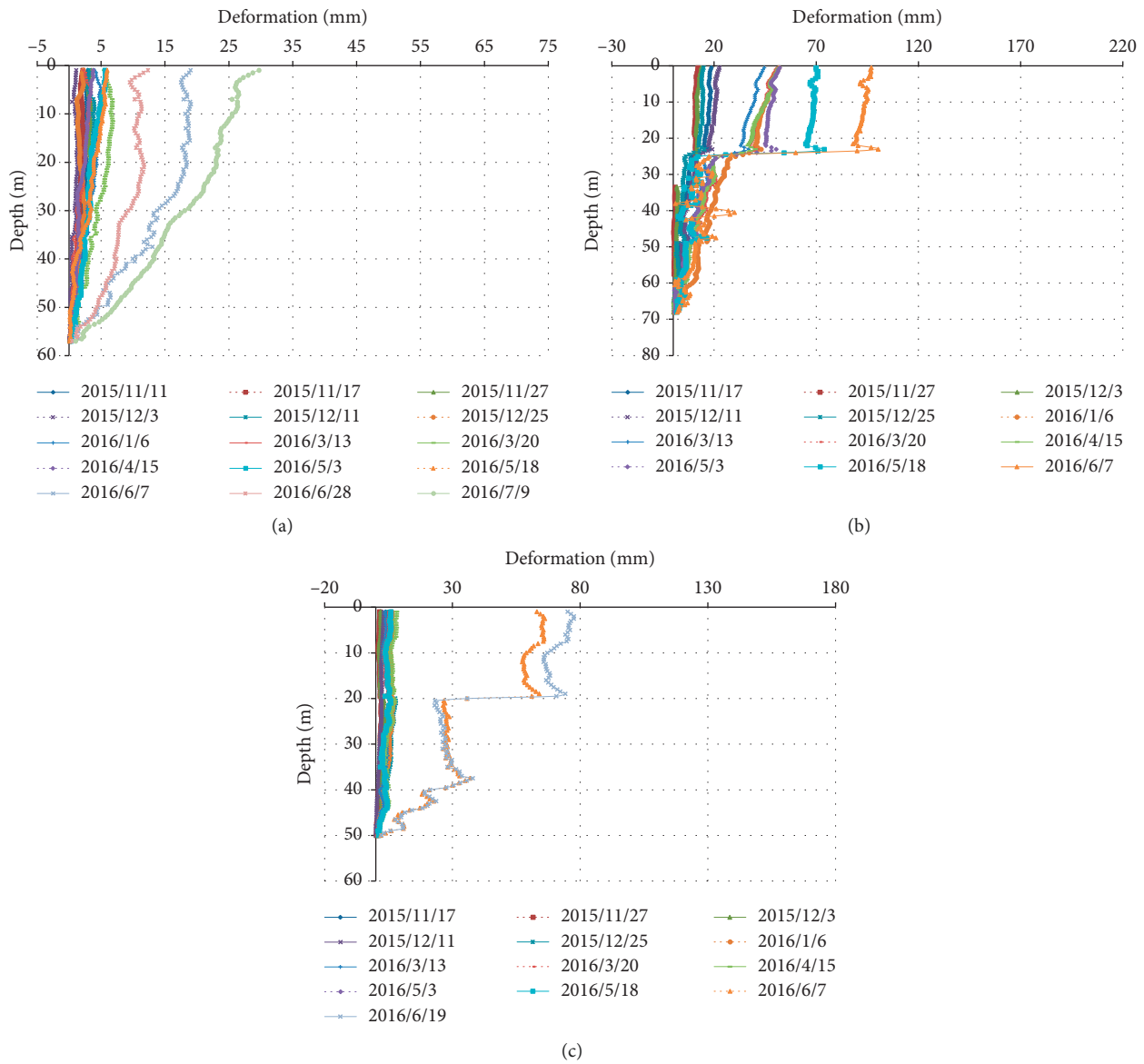

Figure 4: Cumulative displacement curve at different elevations for the inclination survey of CJQ-3-3 section. (a) Elevation 1,710 m. (b) Elevation 1,660 m. (c) Elevation 1,560 m.

suggested by geotechnical engineer, as listed in Table 2.

(4) The four-level parameters of c and ϕ should be quartering values of the minimum and maximum values of strength parameters determined above.

The minimum and maximum values of c and ϕ determined according to the above mentioned principles, respectively, are c_c (17.86~19.42 kPa) and ϕ_c (18.00°~19.46°) for Cangjiangqiao landslide and c_d (17.48~20.14 kPa) and ϕ_d (21.08°~23.95°) for Dahua landslide; 16 groups of c and ϕ for the two-parameter and four-level method for Cangjiangqiao and Dahua landslides are determined, respectively (see Tables 3 and 4).

4.3. Back Analysis on Strength Parameters. According to the typical geological profiles of Cangjiangqiao and Dahua landslides in Figures 2(a) and 2(b), the corresponding 2D finite element models (see Figure 6) are established. In the 2D modeling, SW293.5° is regarded as the positive direction of x-axis and the upward direction is the positive direction of y-axis; z-axis was identified by the right-hand rule, and thickness was set to be 2 m. The Cangjiangqiao model, which is 1120 m $(x) \times 480$ m $(y) \times 2$ m (z) in dimension, is composed of 8,417 regular hexahedral elements and 17,344 nodes (see Figure 6(a)). The Dahua model, which is 1180 m $(x) \times$ 580 m $(y) \times 2$ m (z) in dimension, is composed of 8, 417 regular hexahedral elements and 17, 344 nodes (see Figure 6(b)). Normal constraint is adopted in the surrounding of models and fixed constraint is adopted at the bottom; slope surface is a free boundary.

In the finite element analysis, displacement values at monitoring points that are the same positions as SN3-2 and SN3-3 for Cangjiangqiao landslide and SAA2-1 and SN3-3

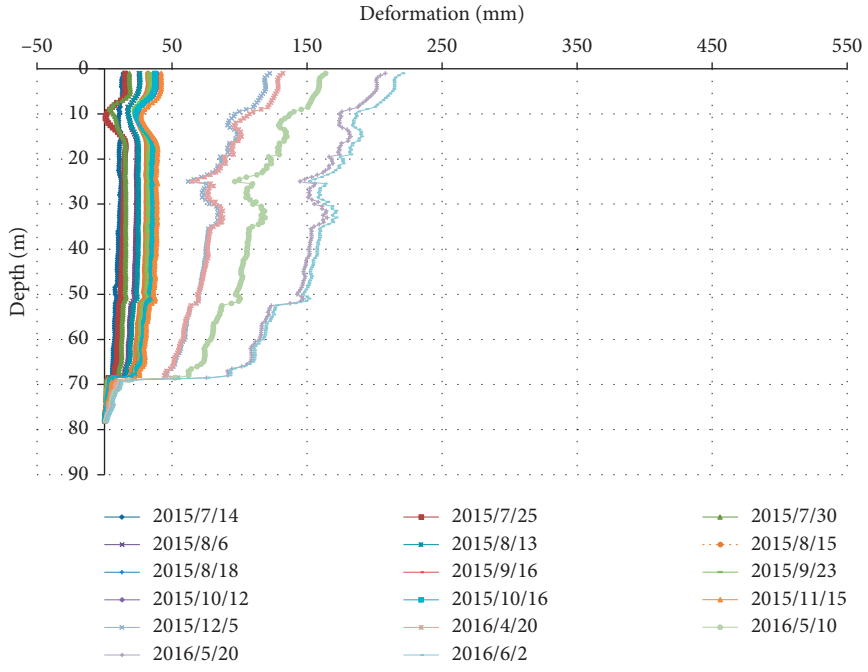

(a)

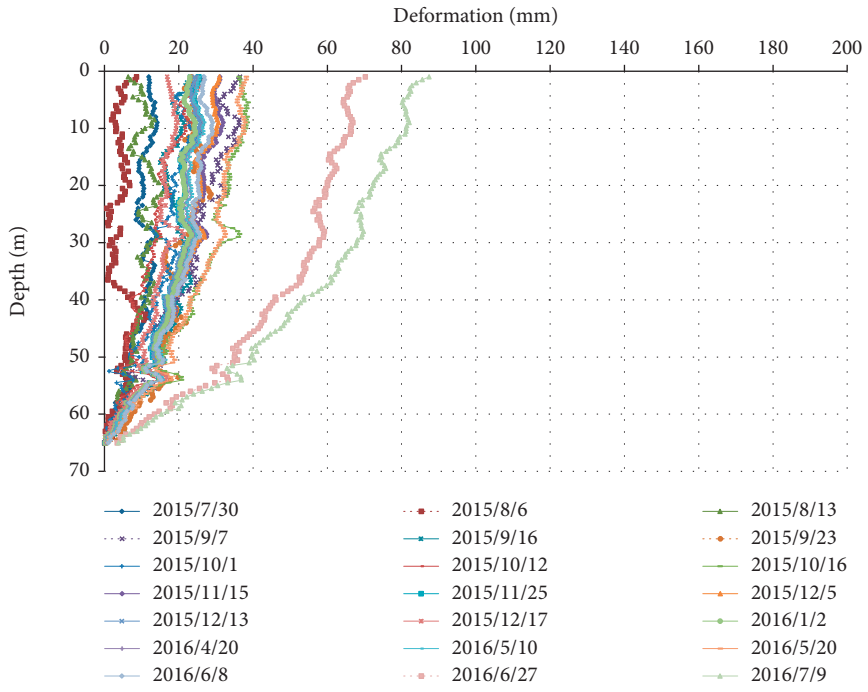

(b)

Figure 5: Continued.

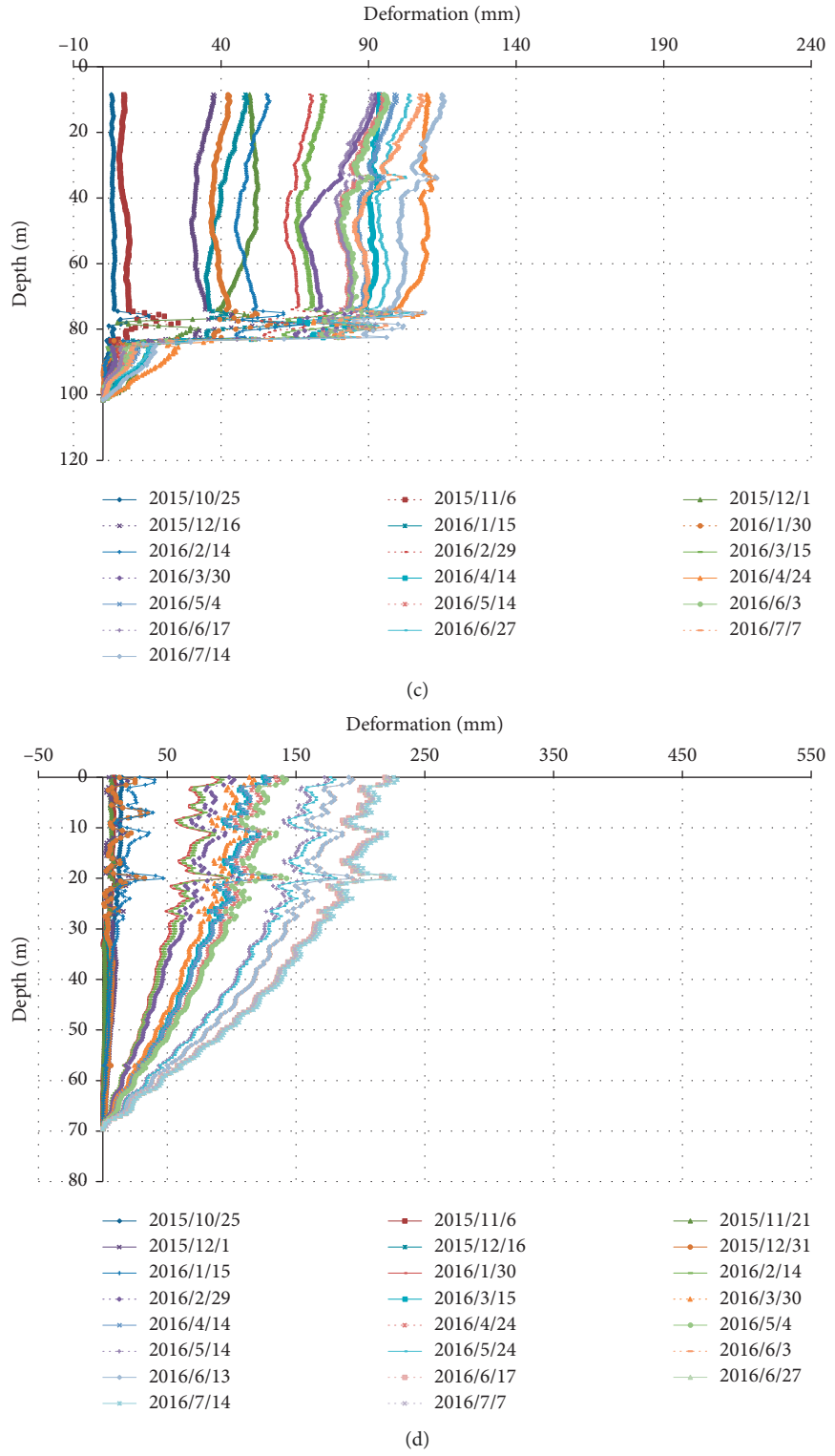

Figure 5: Cumulative displacement curve at different elevations for the inclination survey of DH-2-2 Section. (a) Elevation 1,710 m. (b) Elevation 1,650 m. (c) Elevation 1,550 m. (d) Elevation 1,480 m.

for Dahua landslide are monitored. These monitoring points are also the location where actual inclinometers are installed. Once the finite element models for two-factor and four-level back analysis method are set, normal finite element calculation by inputting each group of selected strength parameters as listed in Tables 3 and 4 and other physical and mechanical parameters as listed in Table 2 is performed. The calculated displacement values at monitoring points SN3-2

Table 2: Physicomechanical parameters for landslides in Dahuaqiao reservoir.

Name	Material type	ϕ (°)	c (kPa)	E (GPa)	ε	γ (kN/m^3)	γ_{sat} (kN/m^3)
Cangjiangqiao	Cover layer	20	20	0.4	0.34	21	22
	Intensely weathered bedrock	33	750	10	0.2	26.6	26.8
	Moderately weathered bedrock	40	2000	30	0.15	27.0	27.2
Dahua	Cover layer	25	22	0.5	0.30	21	22
	Intensely weathered bedrock	33	750	10	0.2	26.6	26.8
	Moderately weathered bedrock	40	2000	30	0.15	27.0	27.2

Table 3: Names of the 16 groups of c and ϕ for Cangjiangqiao landslide.

		Cohesion (kPa)			
		19.42	18.87	18.35	17.86
Internal friction angle (°)	19.46	CJQ 1-1	CJQ 1-2	CJQ 1-3	CJQ 1-4
	18.95	CJQ 2-1	CJQ 2-2	CJQ 2-3	CJQ 2-4
	18.47	CJQ 3-1	CJQ 3-2	CJQ 3-3	CJQ 3-4
	18.00	CJQ 4-1	CJQ 4-2	CJQ 4-3	CJQ 4-4

Table 4: Names of the 16 groups of c and ϕ for Dahua landslide.

		Cohesion (kPa)			
		20.14	19.14	18.97	17.48
Internal friction angle (°)	23.95	DHQ 1-1	DHQ 1-2	DHQ 1-3	DHQ 1-4
	22.88	DHQ 2-1	DHQ 2-2	DHQ 2-3	DHQ 2-4
	21.99	DHQ 3-1	DHQ 3-2	DHQ 3-3	DHQ 3-4
	21.08	DHQ 4-1	DHQ 4-2	DHQ 4-3	DHQ 4-4

and SN3-3 for Cangjiangqiao and SAA2-1 and SN3-3 for Dahua for each group of strength parameters of slip surface are obtained (see Tables 5 and 6).

Generally, displacements at monitoring points are dependent upon the physical properties of the sliding mass and slip surface, and the function of these parameters is

$$X_i = f\left(c_s, \phi_s, E_s, c_m, \phi_m, E_m, \ldots\right), \tag{1}$$

where c_s, ϕ_s, and E_s are, respectively, cohesion, friction angle, and elastic modulus associated with the slip surface and c_m, ϕ_m, and E_m are cohesion, friction angle, and elastic modulus of sliding mass. In the following analysis, only c_s and ϕ_s in equation (1) are variables, and other physical parameters are constants. The functional relation of equation (1) for a series of calculated displacement values at one monitoring point can be determined by the multivariable nonlinear regression analysis which is commonly imbedded in commercial software like Matlab. Among the four monitoring points SN3-1, SN3-2, SN3-3, and SAA3-1 in Figure 6(a), SN3-1 and SAA3-1 have no obvious deformation in the monitoring process; thus, only the calculated displacement values of SN3-2 and SN3-3 (see Table 5) are used to determine the values of cohesion and friction angle during the back analysis. The relationships of calculated displacements with combinations of c_s and ϕ_s can be obtained by using the data in Table 5 and indicated, respectively, by curves L_1 and L_2 for monitoring points SN3-2 and SN3-3 as shown in Figure 7. Obviously, it is difficult to determine an exact solution of c_s and ϕ_s that simultaneously satisfy the two curves L_1 and L_2; therefore, an optimal solution of c_s and ϕ_s is searched by using the least error of displacement difference for these curves at two monitoring points SN3-2 and SN3-3.

Generally, the error in the two-parameter and four-level method is defined as the relative difference between the calculated displacement and the measured one, as shown in the following equation:

$$e_{i,j}^k = \frac{d_{i,j}^k - d^k}{d^k}, \tag{2}$$

where i is level number of cohesion c_s, $i = 1, 2, 3, 4$; j is the level number of friction angle ϕ_s, $j = 1, 2, 3, 4$; k is the number of monitoring points; d^k is the measured displacement value at monitoring point (for example, SN3-2 or SN3-3); and d_{ij}^k is the calculated displacement value at monitoring point of k at c_{si}, ϕ_{sj} by using finite element analysis.

The solution domain is divided by different combinations of c_s ($i = 1, 2, 3, 4$) and ϕ_s ($j = 1, 2, 3, 4$) into nine subdomains V_{ij} ($i = 1, 2, 3$; $j = 1, 2, 3$), as shown in Figure 7. The domain error eV_{ij} associated with displacement values can be determined by the error at monitoring points:

$$eV_{ij} = \sum_{k=1}^{n} e_{i,j}^k + e_{i+1,j}^k + e_{i,j+1}^k + e_{i+1,j+1}^k, \tag{3}$$

where n is the number of monitoring points. The subdomain where eV_{ij} is the minimum is optimal one where the most possible combination of c_s and ϕ_s gives the measured displacements at monitoring points. Once the optimal subdomain is determined, the error e at the arbitrary point in this domain can be obtained based on the point's distance to the four corners of this subdomain as shown in Figure 7:

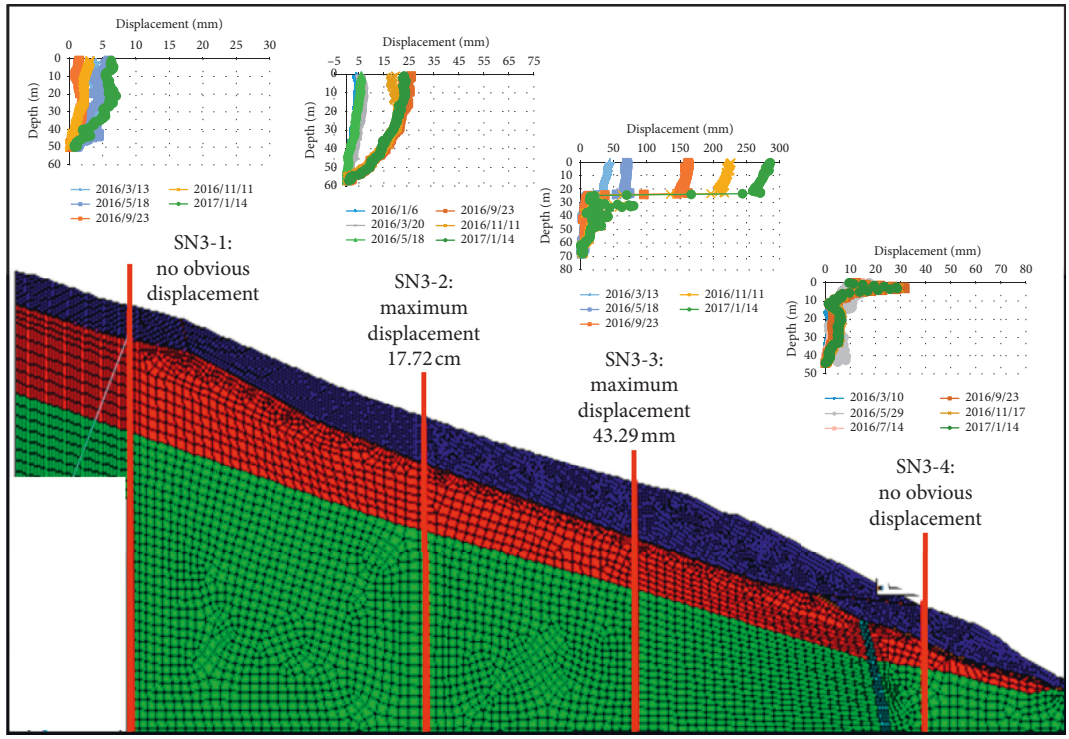

(a)

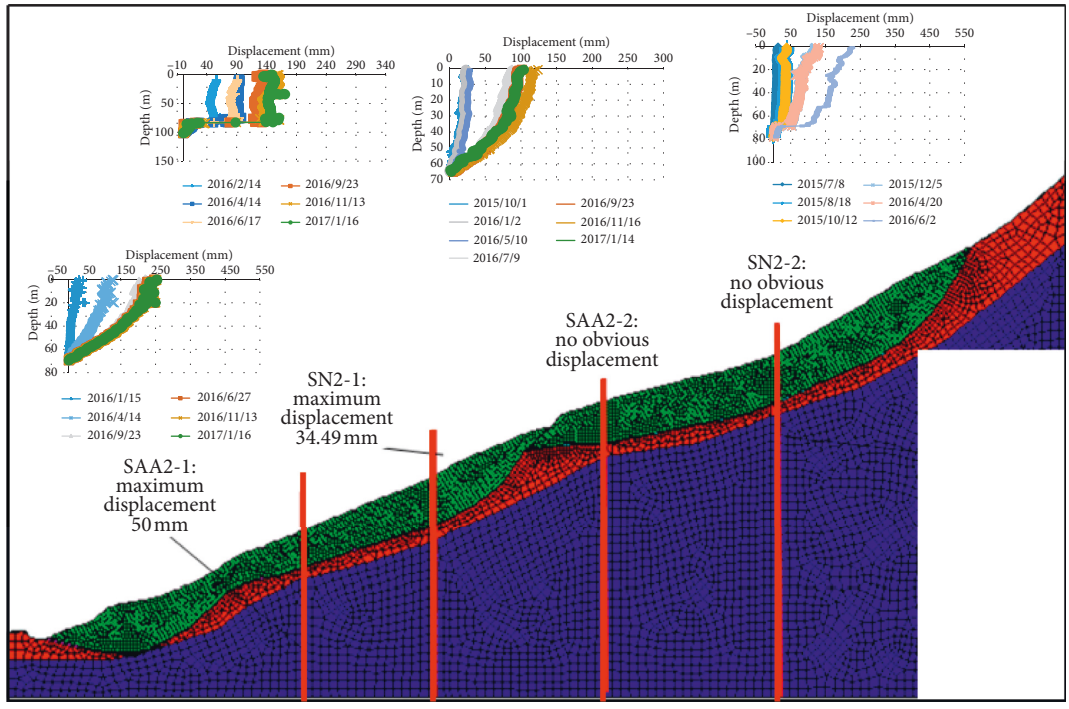

(b)

Figure 6: Finite element back analysis models for typical landslide sections. (a) Cangjiangqiao landslide. (b) Dahua landslide.

$$e = \sum_{k=1}^{n} \frac{e_{i,j}^{k}(r_1 + r_2) + e_{i+1,j}^{k}(1 - r_1 + r_2) + e_{i,j+1}^{k}(r_1 + 1 - r_2) + e_{i+1,j+1}^{k}(2 - r_1 - r_2)}{2}, \tag{4}$$

Table 5: Calculated deformation values of Cangjiangqiao landslide (mm).

		Cohesion (kPa)				
		19.42	18.87	18.35	17.86	
Internal friction angle (°)	19.46	10.1	12.0	13.8	15.2	Cangjiangqiao SN3-2
	18.95	24.3	30.8	36.2	42.2	
	18.47	27.5	43.2	56.3	69.8	
	18.00	48.9	61.7	79.2	365.1	
Internal friction angle (°)	19.46	12.6	15.4	16.8	18.4	Cangjiangqiao SN3-3
	18.95	29.2	38.2	43.8	52.4	
	18.47	33.2	52.8	67.8	85.2	
	18.00	58.8	74.6	95.2	373.5	

Table 6: Calculated deformation values of Dahua landslide (mm).

		Cohesion (kPa)				
		20.14	19.14	18.97	17.48	
Internal friction angle (°)	23.95	33.5	41.1	46.0	47.8	Dahua SAA2-1
	22.88	47.6	52.3	54.4	56.3	
	21.99	57.9	59.2	61.3	63.9	
	21.08	65.2	66.9	69.4	No converge	
Internal friction angle (°)	23.95	25.7	30.7	34.4	36.1	Dahua SN2-1
	22.88	36.2	39.1	41.3	42.5	
	21.99	44.0	44.8	46.4	48.2	
	21.08	49.2	50.7	52.0	No converge	

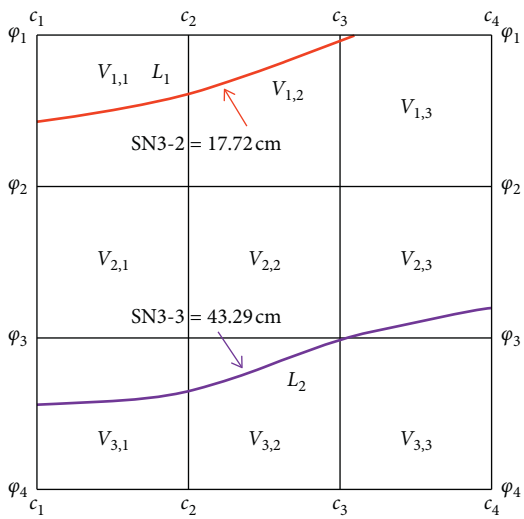

Figure 7: Conceptual diagram of deformation with strength parameters.

where r_1 and r_2 are upward percentages of c and ϕ away from the minimum values in the optimal subdomain. Once the minimum of e is obtained, the final solution to c_s and ϕ_s can be calculated through the following equation:

$$c = c_i + (\phi_{i+1} - \phi_i) * r_1,$$
$$\phi = \phi_j + (\phi_{j+1} - \phi_j) * r_2. \quad (5)$$

Similarly, two series of calculated displacement values at monitoring points SAA2-1 and SN2-1 for Dahua landslide are used (see Table 6). The final back-analyzed values of cohesion and friction angle for actual deformation state at Cangjiangqiao and Dahua landslides are summarized in Table 7.

Based on the back analysis results of strength parameters of slip surface (see Table 7), the finite element analysis is conducted on Cangjiangqiao and Dahua landslides, and the corresponding displacement contour is shown in Figure 8. The recalculated displacements by using the back-analyzed parameters for Cangjiangqiao and Dahua landslides are presented in Table 7. It can be found from Figure 8 and Table 8 that the relative difference between the measured displacement and that calculated based on the back-analyzed strength parameters of slip surface is within 2%. It indicates that the two-parameter and 4-level method is feasible for back analyzing the strength parameters of the measured displacements.

5. Slope Stability Analysis for Cangjiangqiao and Dahua Landslides

5.1. Establishment of the Stability Model. According to shear strength parameters determined by back analysis of displacement, the stability analysis of Cangjiangqiao and Dahua landslides before and after the impoundment is performed by using two-dimensional rigid body limit equilibrium method and then reinforcement measures are proposed. According to Chinese Design Specification for Slope of Hydropower and Water Conservancy Project [21], Cangjiangqiao and Dahua landslides are classified as reservoir slopes of Category B at Level II due to their location. When the stability is analyzed using the limit equilibrium method, the minimum factors of safety for natural state, rainfall, and earthquake conditions should be 1.15 to 1.05, 1.10 to 1.05, and above 1.00, respectively (see Table 9).

Table 7: Back analysis results for strength parameters.

Landslide	Initial parameters		Lower bound of parameters		Results determined by back analysis	
	ϕ (°)	c (kPa)	ϕ (°)	c (kPa)	ϕ (°)	c (kPa)
Cangjiangqiao	19.00	10.00	16.63	8.62	17.60	9.50
Dahua	23.95	20.14	21.08	17.48	23.40	17.80

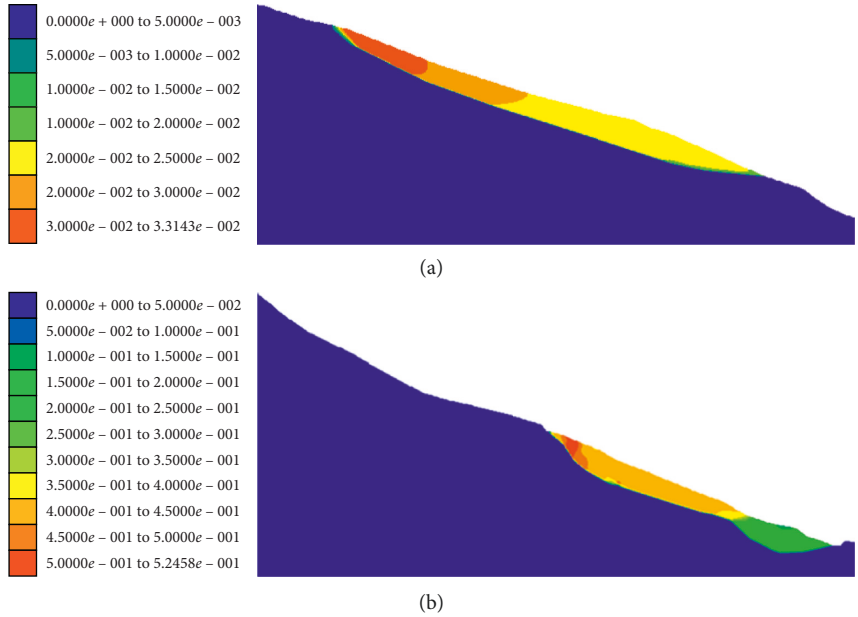

Figure 8: Finite element analysis based on the back analysis results. (a) Cangjiangqiao. (b) Dahua.

Table 8: Comparison of measured displacement with that obtained based on the back-analyzed strength parameters of slip surface.

	Cangjiangqiao		Dahua	
Monitoring point	SN3-3	SN3-2	SAA2-1	SN2-1
Measured result (mm)	17.72	43.29	50.00	34.49
Inversion result (mm)	18.01	42.89	48.72	34.87
Relative error (%)	1.64	−0.92	−2.56	1.10

Table 9: Calculated factors of safety for Canjianqiao and Dahua landslides.

Landslide		Calculation conditions			
		Natural state	Precipitation	Earthquake	Drawdown
Cangjiangqiao	Before impoundment	1.07	1.04	0.98	—
	After impoundment	1.09	1.08	0.99	1.06
	After impoundment with prestressed anchor cables	1.09	1.09	1.00	1.07
Dahua	Before impoundment	1.08	1.04	0.99	—
	After impoundment	1.07	1.04	0.98	1.06
	After impoundment with antisliding piles	1.09	1.06	1.00	1.09
Allowable factor of safety		1.15~1.05	1.10~1.05	1.00	1.10~1.05

5.2. Stability Analysis. Slope stability was analyzed according to the geological profile, parameters back analyzed, and monitoring results mentioned above. The analysis results and the calculation diagram of Cangjiangqiao and Dahua landslides are shown in Table 9 and Figures 9 and 10, respectively.

It can be known from Table 9 and Figures 9 and 10 that the factor of safety in the case of earthquake is slightly lower

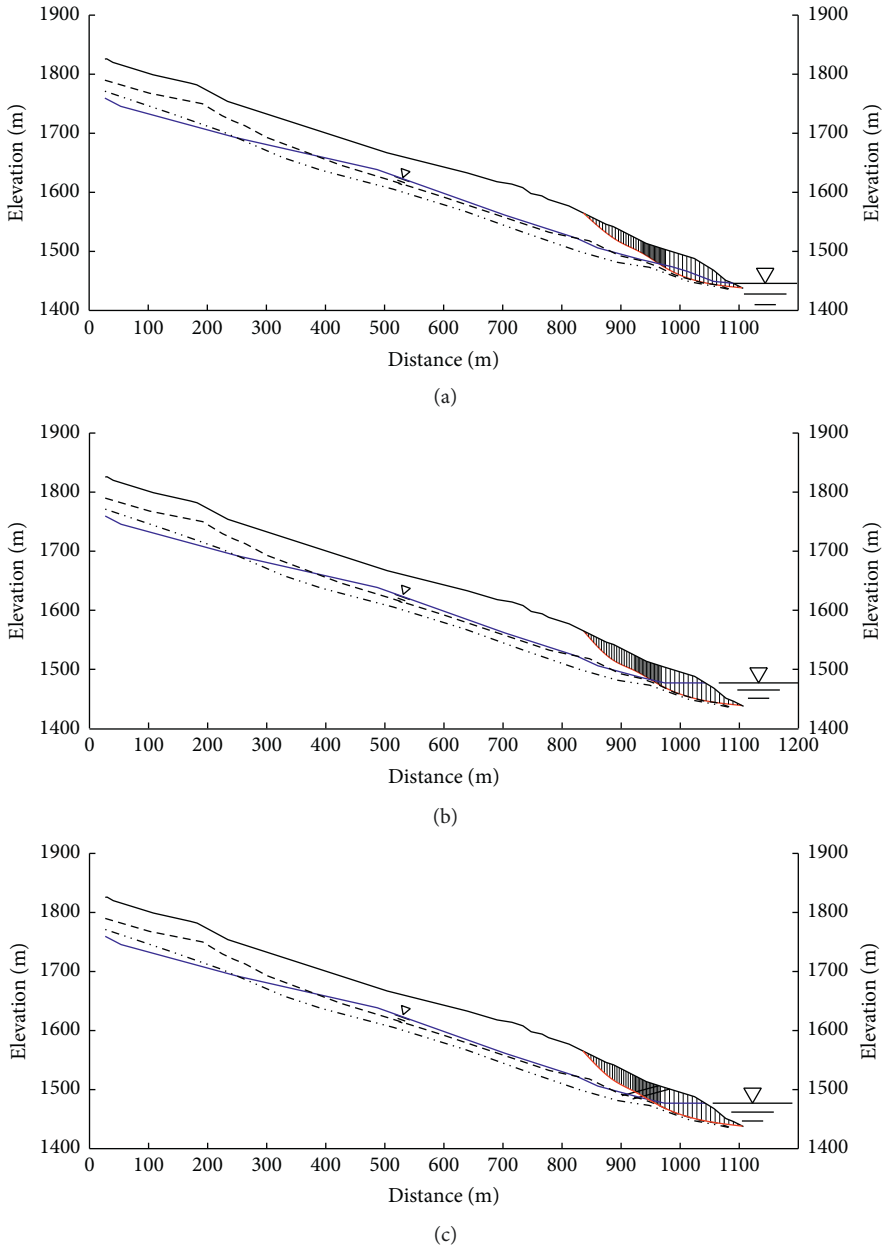

Figure 9: Stability analysis results and diagram of Cangjiangqiao landslide subject to earthquake. (a) Before impoundment. (b) After impoundment without stabilization measures. (c) After impoundment with stabilization measures.

than that specified by national specification of slope stability [18], indicating that earthquake is a governing case for the stability of Cangjiangqiao and Dahua landslides. In combination with the engineering geological conditions of landslide masses and engineering experience, the reinforcement measure of drainage combined with piles will be adopted. The stability analysis results after considering remedial measures are shown in Table 9, and its calculation diagrams are shown in Figures 9 and 10. As shown in Table 9, the factors of safety after adopting drainage and piles meet the stability standard, and slope drainage has a remarkable influence on the stability of landslide masses. By using stability analysis strategy, stability of landslides in the Dahuaqiao reservoir area is revaluated and appropriate engineering measures are suggested. No obvious instable or adverse failures are found in the reservoir area after impoundment.

6. Conclusions

(1) The slope deformation monitoring data indicate that creep and deep deformation is the major deformation pattern for slope failures found in the Dahuaqiao reservoir area. The spatiotemporal evolution of deep displacement decreases with depth, but increases with time. The deep displacement of

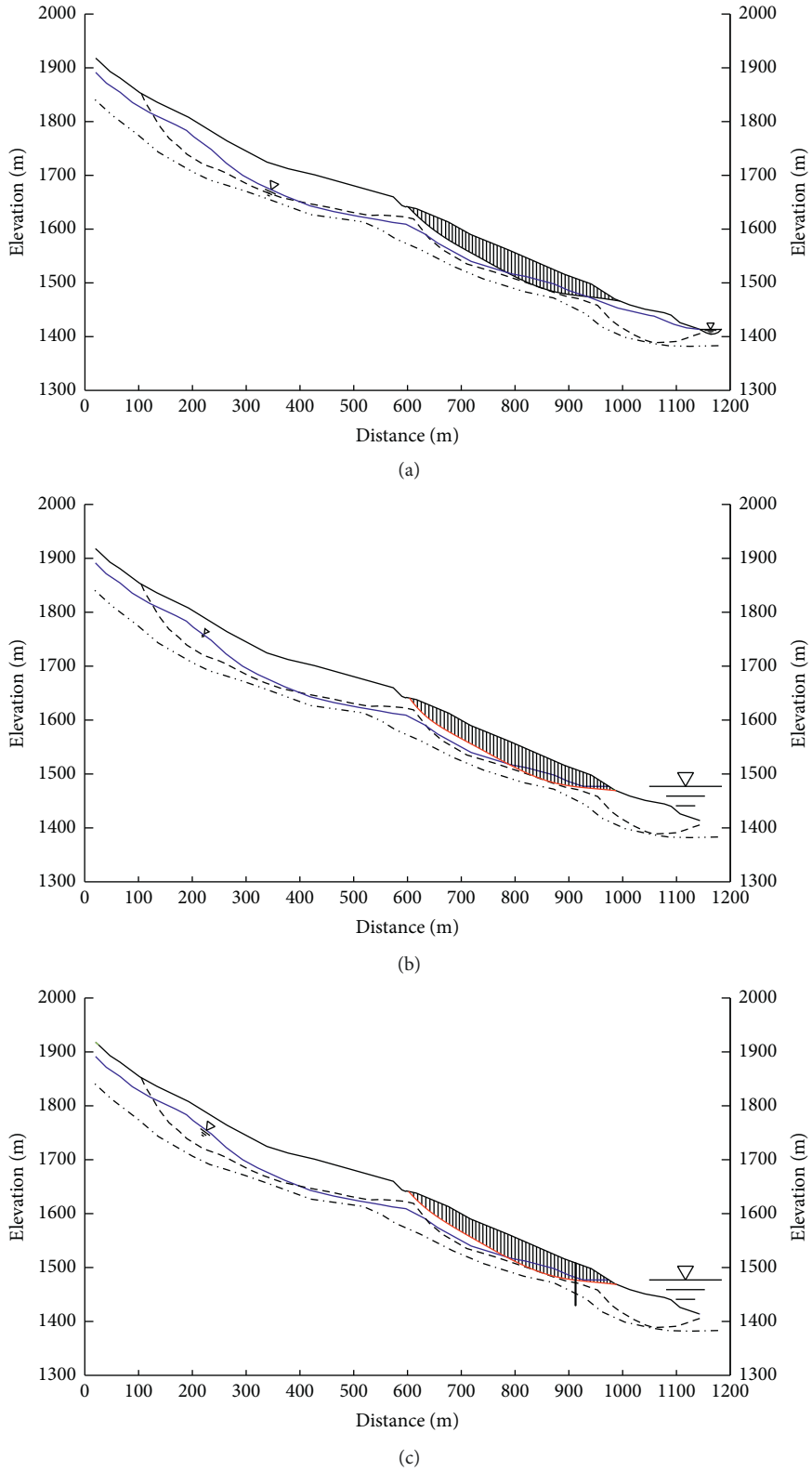

Figure 10: Stability analysis results and diagram of Dahua landslide subject to earthquake. (a) Before impoundment. (b) After impoundment without stabilization measures. (c) After impoundment with stabilization measures.

those slope failures is greatly affected by precipitation and will be worsened by reservoir water level fluctuation.

(2) The strength parameters associated with slip surface based on deformation monitoring results were fitted by using the two-parameter and four-level back analysis method proposed in the present paper.

(3) Stability effects of remedial measures, such as drainage, ground anchors, and piles against sliding in different operating conditions, were assessed based on the rigid body limit equilibrium method and the back-analyzed parameters. Finally, a treatment scheme composed of internal drainage within the slope and piles against sliding was proposed.

Data Availability

The monitoring data used to support the findings of this study are included within the article.

Conflicts of Interest

The authors declare that they have no conflicts of interest.

Acknowledgments

This work was supported by grants from the National Key R&D Project of China (grant nos. 2017YFC1501103 and 2018YFC0407003) and the Fundamental Research Funds Project of China Institute of Water Resources and Hydropower Research (grant no. GE0145B822017).

References

[1] L. Muller, "The rock slide in the Vajont Valley," *Rock Mechanics and Rock Engineering*, vol. 2, pp. 148–212, 1964.

[2] ICOLD (International Commission on Large Dams), *Reservoir landslides: Investigation and Management—Guidelines and Case Histories*, vol. 124, Bulletin, Paris, France, 2002.

[3] M. Saito, "Forecasting the time of occurrence of a slope failure," in *Proceedings of the 6th International Conference on Soil Mechanics and Foundatin Engineering*, pp. 537–541, Montreal, QC, Canada, September 1965.

[4] L. Lfieri, P. Salamon, F. Pappenberger, F. Wetterhall, and J. Thielen, "Operational early warning systems for water-related hazards in Europe," *Environmental Science & Policy*, vol. 21, pp. 35–49, 2012.

[5] G. Capparelli and D. Tiranti, "Application of the MoniFLaIR early warning system for rainfall-induced landslides in Piedmont region (Italy)," *Landslides*, vol. 7, no. 4, pp. 401–410, 2010.

[6] G. Capparelli and P. Versace, "FLaIR and SUSHI: two mathematical models for early warning of landslides induced by rainfall," *Landslides*, vol. 8, no. 1, pp. 67–79, 2011.

[7] G. Capparelli, P. Iaquinta, G. G. R. Iovine, O. G. Terranova, and P. Versace, "Modelling the rainfall-induced mobilization of a large slope movement in northern Calabria," *Natural Hazards*, vol. 61, no. 1, pp. 247–256, 2012.

[8] R. K. Dahal, S. Hasegawa, A. Nonomura, M. Yamanaka, S. Dhakal, and P. Paudyal, "Predictive modelling of rainfall-induced landslide hazard in the Lesser Himalaya of Nepal based on weights-of-evidence," *Geomorphology*, vol. 102, no. 3-4, pp. 496–510, 2008.

[9] M. Galli, F. Ardizzone, M. Cardinali, F. Guzzetti, and P. Reichenbach, "Comparing landslide inventory maps," *Geomorphology*, vol. 94, no. 3-4, pp. 268–289, 2008.

[10] F. Guzzetti, S. Peruccacci, M. Rossi, and C. P. Stark, "The rainfall intensity-duration control of shallow landslides and debris flows: an update," *Landslides*, vol. 5, no. 1, pp. 3–17, 2008.

[11] G. Q. Chen, R. Q. Huang, H. Zhou et al., "Research on progressive failure for slope using dynamic strength reduction method," *Rock and Soil Mechanics*, vol. 34, no. 4, pp. 1140–1146, 2013, in Chinese.

[12] J. S. Chen, C. X. Chen, H. B. Zhao et al., "Research of landslide pre-warning based on Fourier Analysis for displacement-time sequence," *Yangtze River*, vol. 44, no. 22, pp. 64–68, 2013, in Chinese.

[13] X. H. He, S. J. Wang, and R. H. Xiao, "Improvement and application of synergetic forecast model for landslides," *Chinese Journal of Geotechnical Engineering*, vol. 35, no. 10, pp. 1839–1848, 2013, in Chinese.

[14] A. Bardoux, C. Graf, J. Rhyner et al., "A debris-flow alarm system for the Alpine Illgraben catchment: design and performance," *Natural Hazards*, vol. 49, pp. 517–539, 2009.

[15] C. Michoud, S. Bazin, L. H. Blikra, M.-H. Derron, and M. Jaboyedoff, "Experiences from site-specific landslide early warning systems," *Natural Hazards and Earth System Sciences*, vol. 13, no. 10, pp. 2659–2673, 2013.

[16] M. Calvello, L. Cascini, and G. Sorbino, "A numerical procedure for predicting rainfall-induced movements of active landslides along pre-existing slip surfaces," *International Journal for Numerical and Analytical Methods in Geomechanics*, vol. 32, no. 4, pp. 327–351, 2007.

[17] B. Han, S. Hou, H. Ye, B. Zhu, and P. Zhou, "Multi-parameter monitoring and deformation mechanism research on a reservoir landslide in Western China," *Electronic Journal of Geotechnical Engineering*, vol. 19, pp. 3615–3622, 2014, http://www.ejge.com/2014/Ppr2014.342mar.pdf.

[18] Y. Gao, F. Zhang, G. H. Lei, D. Li, Y. Wu, and N. Zhang, "Stability charts for 3D failures of homogeneous slopes," *Journal of Geotechnical and Geoenvironmental Engineering*, vol. 139, no. 9, pp. 1528–1538, 2013.

[19] F. Zhang, D. Leshchinsky, R. Baker, Y. Gao, and B. Leshchinsky, "Implications of variationally derived 3D failure mechanism," *International Journal for Numerical and Analytical Methods in Geomechanics*, vol. 40, no. 18, pp. 2514–2531, 2016.

[20] J. Ji, C. Zhang, Y. Gao, and J. Kodikara, "Effect of 2D spatial variability on slope reliability: a simplified FORM analysis," *Geoscience Frontiers*, vol. 9, no. 6, pp. 1631–1638, 2018.

[21] China Electric Power Press, *Design Specification for Slope of Hydropower and Water Conservancy Project, (DL/T. 5353-2006)*, China Electric Power Press, Beijing, China, 2006, in Chinese.